

A DIGITAL PHOTOGRAMMETRIC SYSTEM FOR THREE-DIMENSIONAL DEFORMATION MEASUREMENT

Weiyang Zhou, Robert Brock, James Thorpe and Paul Hopkins
SUNY College of Environmental Science and Forestry
Syracuse, NY 13210

ABSTRACT:

A self-calibrating digital photogrammetric system is employed to determine three dimensions in object space. Digital imagery is collected by two Panasonic WV-CD20 CCD cameras at a distance of about 26 inches from the object specimen. The image coordinates of control placed in the object space are measured from a monitor. The image coordinates of random dots placed on the specimen are determined using a feature-based image matching procedure. A photogrammetric bundle adjustment method constrained by weights on appropriate variables provides the solution for all parameters including the object coordinates of the random dots on the specimen. Results to date indicate that average standard deviations in inches for the random dots are 0.006, 0.006, and 0.027 respectively, for X, Y, and Z.

KEY WORDS: digital photogrammetry, close-range, self-calibrating, stereo-pair image matching, 3-D reconstruction, bundle adjustment.

1. INTRODUCTION

In solid mechanics the surface of a specimen will deform when force is applied to it. The present analysis of this deformation utilizes a linear image strain analysis system, LISA, which is able to detect and measure the displacement in two orthogonal directions (X and Y) in the plane of the surface of the specimen. Usually the measured directions are across and along the direction of applied force.

The purpose of an ongoing project is to develop a non-contact digital image acquisition and analysis system to quantify the deformation in three dimensions. This paper reports on the progress of this project to date.

2. BACKGROUND

The principles of photogrammetry have long been used in non-topographical measurement [4] [7]. With the advent of digital sensors digital images are being used as information sources instead of photos. In comparison with traditional hard copy photos digital images have the advantage of being highly computer-compatible. With the ever-increasing power and availability of computers and data sources, and the increasing need for real time processing, digital image processing and analysis has become an inseparable part of analytical photogrammetry. By using digital cameras some of the errors associated with the traditional methods can be avoided, such as those introduced by the deformation of the film negative during the procedure of developing and drying.

The use of non-metric digital cameras requires that a self-calibration procedure be used. Generally CCD (charge coupled device) cameras have no fiducial marks and the location of the principal point must be calculated. The CCD camera may use different lenses for different applications and thus require calibration for each use. Likewise the principal distance of the CCD camera used for close-range work is constantly changing and its determination must be made for each image processed.

Often in the use of self-calibrating bundle adjustments the camera station parameters are of no real interest [7]. Generally one is concerned with the object point coordinates and their error estimates.

Most photogrammetric techniques are based on the geometric relationships between the object's position in the object space and its position on the surface of the sensitive recording part (i.e., the negative film with the traditional camera and the CCD chip with the CCD camera) of the sensor. The position of an object point, after projection onto the surface of the sensor of the CCD camera, is unknown and cannot be measured directly as with the traditional negatives. The position of the image in the sensor plane must be determined in terms of pixel coordinates. The actual space represented by one pixel is critical to the success of the data reduction. The actual ability to measure coordinates in CCD cameras is often + 0.015 mm. whereas this typically is + 0.005 mm. in terms of film based cameras. This difference between the camera systems in coordinate measurement capability will decrease as CCD technology advances.

3. THE EXPERIMENT

3.1 Objective

The objective of this study is to develop a digital self-calibrating analytical photogrammetric procedure to determine the three-dimensional spatial coordinates of random points on a surface whose image positions are automatically determined through image matching techniques. Figure 1 shows a schematic diagram of the experimental setup.

3.2 Hardware

The layout of the computer image analysis system is as shown in Fig. 2. It consists of the components listed below.

1. The host computer. A SUN SPARC system 330 with 16Mbyte memory, SunOS 4.1 operating system and a 1/4 in tape drive.

2. Androx ICS-400 system with 2Mbyte video memory, an extensive library of C-callable graphics and digital signal processing functions.

3. Two Panasonic WV-CD20 CCD cameras with a resolution of 560 by 482 (8.8 mm by 6.6 mm image field) pixels and changeable lenses.

4. A NEC Multisync color monitor.

3.3 General Procedure

The experimental procedure can be summarized in the five following steps.

1. For this experiment, the control/test model consists of ten precision machine blocks whose dimensions are known. The size of the model is approximately 6 by 6 by 4 inches. The CCD cameras are positioned about 7 inches apart and about 26 inches above the model. Multiple images are taken with both cameras under various illumination conditions.

2. Using the image displayed on the monitor for each camera, determine the image coordinates of the control points on the surface of the model whose object coordinates were previously determined. For the purpose of easy and accurate recognition, a set of well-distributed corners of the blocks were selected. A C-language program, which uses various digital signal processing functions of the Androx system with operator's interactive instructions, was developed for determining the coordinates of the chosen points.

3. Using both cameras, images were taken of a surface of random dots which was superimposed upon the control model as shown in Fig. 3. The illumination should be carefully arranged so that both cameras receive approximately the same amount of exposure. For the purpose of noise reduction, more than one image is taken and averaged.

4. The images containing the random dots were matched. The image coordinates of the dots resulting from the matching process were then placed into the same input data file which contains the image coordinates of the object control points.

5. The bundle adjustment program was executed on the input data files using different weight constraints on particular variables. As a result the object coordinates of the model points, as well as those of the dots on the surface of the specimen, were determined.

3.4 Computational Procedures

The chief computational procedures utilized during the experiment included the self-calibrating analytical photogrammetry bundle adjustment method and the image matching method which was used to determine the image coordinates of the random dots.

3.4.1. Bundle Adjustment Method. This solution was patterned after Brown [10], [11]. Contributions to the

program were made by Orrin Long, Marquess Lewis and Mark Nebrich. The software was modified by Weiyang Zhou for this application.

The basis for the solution is the collinearity equations as follows:

$$F_x = x_s - x_{pp} + f \left[\frac{m_{11}(X_j - X_{ic}) + m_{12}(Y_j - Y_{ic}) + m_{13}(Z_j - Z_{ic})}{m_{31}(X_j - X_{ic}) + m_{32}(Y_j - Y_{ic}) + m_{33}(Z_j - Z_{ic})} \right]$$

$$F_y = y_s - y_{pp} + f \left[\frac{m_{21}(X_j - X_{ic}) + m_{22}(Y_j - Y_{ic}) + m_{23}(Z_j - Z_{ic})}{m_{31}(X_j - X_{ic}) + m_{32}(Y_j - Y_{ic}) + m_{33}(Z_j - Z_{ic})} \right]$$

Where m is a function of camera orientation angles ω , ϕ , and κ and X_{ic} , Y_{ic} and Z_{ic} provide the camera's position in object space. X_j , Y_j and Z_j are the coordinates of point j in the object coordinate system. Interior orientation parameters are represented by f , x_{pp} , and y_{pp} . The image coordinates are x_s and y_s .

Using a linearized version of these two equations for each image point a least squares solution provided all of the parameters and object coordinates after sufficient iterations.

The project efforts are currently experimenting with the expansion of the self-calibration techniques through the incorporation of additional parameters which affect the image coordinates.

3.4.2. Matching Method. Image-matching methods fall into two groups. With the area-based methods, such as [2] and [6], two windows of pixels, one on each image of the pair, are judged to be a match or not according to the similarity between the intensities of the pixels within the two windows. The similarity is determined by calculating statistical values, making these methods statistical by nature. The second group of image matching methods is based on feature, usually edge, information of images [3] [5] [9]. The form and distribution of the features in images are used instead of absolute intensities of the pixels.

It is now generally agreed that edge-based methods have advantages over the area-based methods because it is more reasonable to match images by the variation of pixel intensities than by absolute values of pixel intensities and it is usually more economical in terms of computing time, though there are some methods for improving the efficiency of area-based methods [8].

In mechanical experiments with paper, since there is usually not much texture on paper surfaces, it has been a common practice to place a random pattern onto the surface to enrich the texture. For example, dots with irregular size and shape are used in many experiments. In this work, these dots serve as targets for feature-based image matching.

In order to measure the deformation, there are two types of matching. 1) The matching of two images taken by the same camera before and after the deformation of the

specimen. 2) The matching of two images taken by the two cameras respectively at the same time. With type 1) matching, the difference of the shapes of the same dot in two images was mainly caused by the deformation. With type 2) matching, the difference is mainly introduced by the angle of projection. However, viewing a dot in the image as a density distribution function, the transformation of one function into the other is mainly one of the translation of both X and Y axes. Therefore, the characteristic parameters used to describe a dot must be, first of all, translation invariants. In this experiment, central moments of the first four orders of each dot were calculated as the dot's signature.

$$\begin{aligned}\mu_{00} &= m_{00}, & \mu_{10} &= \mu_{01} = 0 \\ \mu_{20} &= m_{20} - \mu_{00}\bar{x}^2 \\ \mu_{11} &= m_{11} - \mu_{00}\bar{x}\bar{y} \\ \mu_{02} &= m_{02} - \mu_{00}\bar{y}^2 \\ \mu_{30} &= m_{30} - 3m_{20}\bar{x} + 2\mu_{00}\bar{x}^3 \\ \mu_{03} &= m_{03} - 3m_{02}\bar{y} + 2\mu_{00}\bar{y}^3 \\ \mu_{21} &= m_{21} - m_{20}\bar{y} - 2m_{11}\bar{x} + 2\mu_{00}\bar{x}^2\bar{y} \\ \mu_{12} &= m_{12} - m_{02}\bar{y} - 2m_{11}\bar{y} + 2\mu_{00}\bar{x}\bar{y}^2\end{aligned}$$

here,
$$\mu_{pq} = \int_{-\infty}^{+\infty} \int_{-\infty}^{+\infty} (x-\bar{x})^p (y-\bar{y})^q f(x,y) dx dy$$

$$m_{pq} = \int_{-\infty}^{+\infty} \int_{-\infty}^{+\infty} x^p y^q f(x,y) dx dy$$

and
$$\bar{x} = m_{10}/m_{00}, \bar{y} = m_{01}/m_{00}$$

In addition to these, size is an important part of the signature of a dot. However, during the experiment, the size, as well as other factors of the signature, changes from image to image, due to both the projection angles and the deformation of the specimen. Fortunately, a valid assumption of this experiment is that the "distortion" of the shape of a dot in two images is always moderate within small intervals of time between image taking during deformation, and with almost identical projection angles, i.e., with the two cameras kept as vertical to the specimen as possible. Therefore, though they are not exactly invariants in all the images, this set of characteristic values, including central moments and size, comprise a reasonably good signature of a dot.

Because of the digital nature of the images, it is easy to see that dots with a larger size have richer signature information. For example, in the extreme case, dots consisting of a single pixel are all the same in shape. For this reason, as the first iteration of image matching, the biggest dots in both images are selected and matched first by their signatures. However, as discussed above, the signature factors are not exactly invariants. As a consequence, the matching obtained only by signature is not absolutely dependable. An angle test is carried out for the matched dots in the first iteration by checking the difference between the angles formed by any three dots in the first image and the angles formed by the three

correspondingly matched dots in the second image. If the difference is not smaller than a predefined threshold, the matching of one pair of the matched dots will be judged as unacceptable and deleted from the list of matched dots. The angle-test for the first iteration must be done very strictly since the matched dots are going to serve as "seeds" in the following iterations of matching.

After the first matching of the largest dots in the image, a window of adjustable size is opened for each of the two matched dots in each image respectively. Other unmatched dots which fall into the window in two images are matched. As in the first matching, at the end of all the dots in a pair of windows, the "angle-test" is carried out to delete the matches with significant difference in the angles. The threshold to determine if the angle difference is tolerable is dynamic. The more similar a pair of dots are in terms of their signature factors, the looser the threshold will be. In other words, the pair of dots that are very different in their signature have to pass very strict tests on the angle they form in order to be a match.

The dots which are matched in the second matching in turn serve as "seeds" in the third iteration of matching, and so on. The matched dots are no longer considered in the following iterations. The entire matching process comes to an end when all the possible pairs of dots are matched.

After the entire matching process, only the heights at the dots, or more precisely, the heights at the center of the dots, will be solved accurately with intersection. The heights of other points, if of interest, will be determined through interpolation.

After matching the dots in the image, the image coordinates are put into the input data file for a least squares adjustment.

4. RESULTS TO DATE

Sample results are listed in Table 1. These results are for a two camera station solution which utilizes three types of object points, namely, object control points, object check points, and object random dots which will define the final surface deformation of the specimen.

The determination of the interior and exterior orientation parameters for each camera were based on seven (7) known points which were located on the surface of the model. For these points the average absolute residuals in inches between known and final adjusted X, Y and Z coordinates were 0.0024, 0.0021, and 0.0006. An additional eight (8) check points were included in the solution. The weights of these points were zero and thus the solution was free to seek the best fit coordinates for these points. The average absolute residuals in inches in X, Y and Z for these points were 0.0295, 0.0301, and 0.0517.

There were no checks on the computed coordinates for the 132 random dots; however, the average standard deviations in X, Y and Z in inches were 0.0062, 0.0062, and 0.0269 for the listed results in Table 1. In general the results in X and Y are better than in the Z direction.

TABLE 1. Results of Digital Photogrammetric Solution

a) Camera Parameters					d) Results for 13 of 132 Random Object Dots (in)			
		Photo 1	Photo 2			Final	Std. Dev.	
Omega (dd)		-0.719	-2.500		Pt. 20	X	3.893	0.006
Phi (dd)		-11.753	10.535			Y	4.103	0.006
Kappa (dd)		1.112	0.813			Z	2.706	0.027
Xic (in)		-2.134	8.434		Pt. 30	X	3.879	0.006
Yic (in)		2.629	2.684			Y	2.270	0.006
Zic (in)		24.728	26.608			Z	3.193	0.026
xpp (mm)		-0.615	0.842		Pt. 40	X	0.917	0.007
ypp (mm)		-0.382	-1.033			Y	1.606	0.006
f (mm)		21.781	23.616			Z	3.304	0.027
					Pt. 50	X	2.938	0.006
						Y	2.776	0.006
						Z	2.982	0.027
					Pt. 60	X	3.304	0.006
						Y	0.711	0.006
						Z	3.559	0.026
					Pt. 70	X	2.422	0.006
						Y	2.952	0.006
						Z	2.917	0.027
					Pt. 80	X	2.617	0.006
						Y	5.431	0.007
						Z	2.275	0.028
					Pt. 90	X	1.858	0.006
						Y	3.081	0.006
						Z	2.860	0.027
					Pt. 100	X	2.874	0.006
						Y	3.683	0.006
						Z	2.733	0.027
					Pt. 110	X	2.331	0.007
						Y	0.165	0.007
						Z	3.702	0.026
					Pt. 120	X	5.954	0.007
						Y	3.739	0.006
						Z	2.939	0.026
					Pt. 130	X	1.800	0.006
						Y	4.324	0.007
						Z	2.495	0.028
					Pt. 140	X	2.574	0.006
						Y	4.376	0.006
						Z	2.534	0.028
b) Object Control Points (in)								
	Known	Final	Residual	Std. Dev.				
Pt. 1								
X	0.000	0.002	-0.0018	0.002				
Y	0.000	-0.002	0.0022	0.002				
Z	4.021	4.022	-0.0012	0.002				
Pt. 2								
X	6.045	6.042	0.0033	0.002				
Y	0.000	-0.003	0.0029	0.002				
Z	4.021	4.021	0.0004	0.002				
Pt. 4								
X	6.045	6.041	0.0040	0.002				
Y	5.026	5.032	-0.0059	0.002				
Z	3.000	3.000	0.0004	0.002				
Pt. 6								
X	4.669	4.671	-0.0017	0.002				
Y	6.026	6.025	0.0010	0.002				
Z	0.353	0.354	-0.0005	0.002				
Pt. 7								
X	1.376	1.375	0.0013	0.002				
Y	5.976	5.976	0.0003	0.002				
Z	0.353	0.354	-0.0003	0.002				
Pt. 9								
X	0.000	0.002	-0.0019	0.002				
Y	5.026	5.027	-0.0013	0.002				
Z	2.000	1.999	0.0006	0.002				
Pt. 13								
X	4.669	4.672	-0.0031	0.002				
Y	5.379	5.379	0.0008	0.002				
Z	3.000	2.999	0.0005	0.002				
c) Object Check Pts. (in)								
	Known	Final	Residual	Std. Dev.				
Pt. 3								
X	6.045	6.101	-0.0559	0.006				
Y	4.000	4.002	-0.0020	0.005				
Z	1.550	1.601	-0.0505	0.021				
Pt. 5								
X	4.669	4.695	-0.0258	0.004				
Y	5.026	5.066	-0.0395	0.004				
Z	3.000	2.956	0.0441	0.017				
Pt. 8								
X	1.376	1.348	0.0277	0.004				
Y	5.026	5.052	-0.0262	0.005				
Z	2.000	1.930	0.0697	0.019				
Pt. 10								
X	0.000	-0.047	0.0471	0.006				
Y	1.750	1.666	0.0843	0.006				
Z	1.376	1.464	-0.0885	0.026				
Pt. 11								
X	0.000	0.023	-0.0233	0.005				
Y	0.759	0.722	0.0369	0.005				
Z	4.021	4.072	-0.0505	0.018				
Pt. 12								
X	6.045	6.036	0.0091	0.005				
Y	0.759	0.717	0.0421	0.005				
Z	4.021	3.973	0.0482	0.017				
Pt. 14								
X	2.750	2.722	0.0279	0.005				
Y	5.976	5.979	-0.0033	0.006				
Z	0.353	0.305	0.0483	0.023				
Pt. 15								
X	3.295	3.314	-0.0190	0.005				
Y	6.026	6.020	0.0062	0.006				
Z	0.353	0.367	-0.0137	0.023				

5. CONCLUSIONS AND AREAS FOR IMPROVEMENT

It is concluded that the overall results are acceptable but can be improved. Efforts will continue to improve the results and move toward a real time test environment.

Areas for improvement include:

1. Develop a more accurate test control model.
2. Seek improvements in appropriate weight constraints.
3. Explore the use of additional parameters in the initial condition equation.
4. Experiment to determine the absolute accuracy of the image matching process for coordinate measurement.

6. REFERENCES

- [1] Alvertos, N., D. Brzakovic, and R.C. Gonzalez. "Camera Geometries for Image Matching in 3-D Machine Vision." *IEEE Trans. on PAMI*, Vol 11, No 9, September, 1989: 897-914.
- [2] Argenti, F. and L. Alparone. "Coarse-to-Fine Least Square Stereo Matching for 3-D Reconstruction." *Electronics Letters*, Vol 26, No 12, June 1990: 812-13.
- [3] Eastman, E.D. and A.M. Waxman. "Using Disparity Functionals for Stereo Correspondence and Surface Reconstruction." *Computer Vision, Graphics, Image Processing*, Vol 39, 1987: 73-101.
- [4] El-Hakim, S.F. "Real-Time Image Metrology with CCD Cameras." *Photogrammetric Engineering and Remote Sensing*, Vol 52, No 11, November 1986: 1757-66.
- [5] Greenfeld, J.S. and A.F. Schenk. "Experiments with Edge-Based Stereo Matching." *Photogrammetric Engineering and Remote Sensing*, Vol 55, No 12, December 1989: 1771-77.
- [6] Hannah, M.J. "A System for Digital Stereo Image Matching." *Photogrammetric Engineering and Remote Sensing*, Vol 55, No 12, December, 1989: 1765-70.
- [7] Karara, H.M., et al. *Non-topographical Photogrammetry*. ASPRS, 1990.
- [8] Keating, T.J., P.R. Wolf, and F.L. Scarpace. "An Improved Method of Digital Image Correlation." *Photogrammetric Engineering and Remote Sensing*, Vol 41, No 8, August 1975: 993-1002.
- [9] Slama, C.C., et al. *Manual of Photogrammetry*. 4th Ed. ASPRS, 1980.
- [10] Brown, D.C. *A Solution to the General Problem of Multiple Station Analytical Stereotriangulation*. RCS TR43, Patrick Air Force Base, Florida, 1958.
- [11] Brown, D.C. "Close-Range Camera Calibration." *Photogrammetric Engineering*, Vol 37, No 8, August 1971: 855-66.

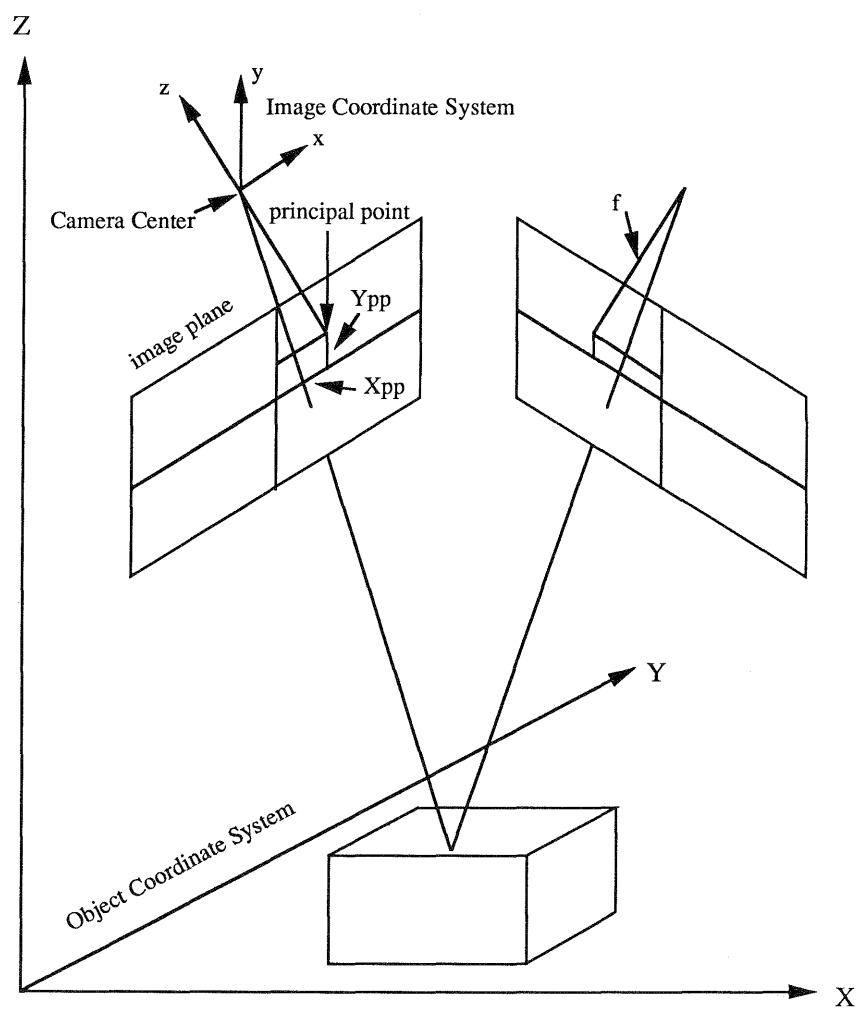


Fig. 1. Schematic diagram of the experiment setup

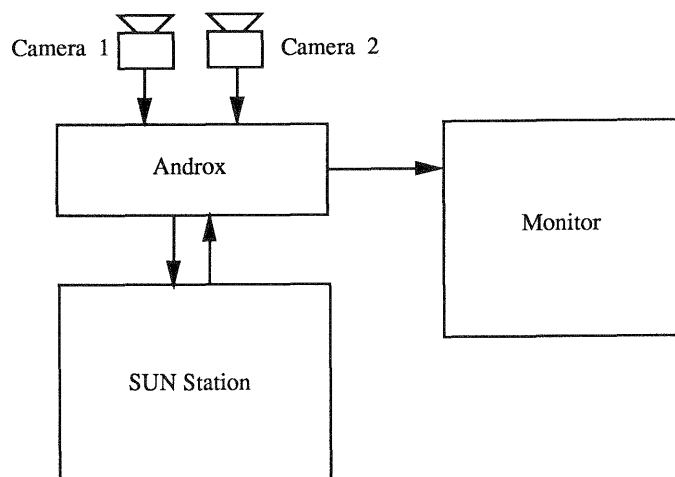


Fig. 2. Layout of the hardware

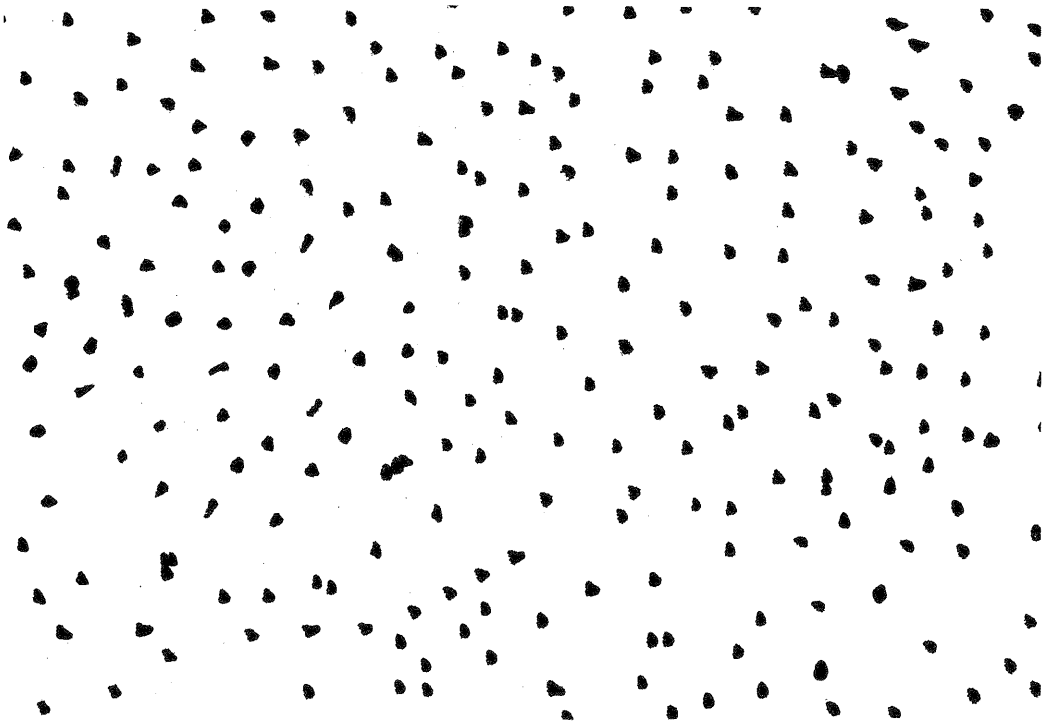


Fig. 3. Example of random-dot surface